

Sequence and electron paramagnetic resonance analyses of nitrate reductase NarGH from a denitrifying halophilic euryarchaeote *Haloarcula marismortui*

Katsuhiko Yoshimatsu^a, Toshio Iwasaki^b, Taketomo Fujiwara^{a,*}

^aDepartment of Biology and Geosciences, Faculty of Science, Shizuoka University, 836 Ohya, Shizuoka 422-8529, Japan

^bDepartment of Biochemistry and Molecular Biology, Nippon Medical School, 1-1-5 Sendagi, Bunkyo-ku, Tokyo 113-8602, Japan

Received 12 December 2001; revised 22 February 2002; accepted 26 February 2002

First published online 6 March 2002

Edited by Hans Eklund

Abstract Genes encoding the NarG and NarH subunits of the molybdo-iron-sulfur enzyme, a nitrate reductase from a denitrifying halophilic euryarchaeote *Haloarcula marismortui*, were cloned and sequenced. An incomplete cysteine motif reminiscent of that for a [4Fe-4S] cluster binding was found in the NarG subunit, and complete cysteine arrangements for binding one [3Fe-4S] cluster and three [4Fe-4S] clusters were found in the NarH subunit. In conjunction with chemical, electron paramagnetic resonance, and subcellular localization analyses, we firmly establish that the *H. marismortui* enzyme is a new archaeal member of the known membrane-bound nitrate reductases whose homologs are found in the bacterial domain. © 2002 Federation of European Biochemical Societies. Published by Elsevier Science B.V. All rights reserved.

Key words: Nitrate reductase; Selenate reductase; Iron-sulfur cluster; Subcellular localization; Electron paramagnetic resonance; *Haloarcula marismortui*

1. Introduction

Denitrifying microorganisms possess nitrate reductase as the terminal enzyme of the nitrate respiration [32]. Except for the enzyme from an anaerobic vanadate-reducing bacterium [4], nitrate reductases generally contain a molybdenum (Mo) atom coordinated with sulfur atoms of a pterin derivative, termed molybdopterin, as the catalytic center. Based on the structural and catalytic properties, dissimilatory nitrate reductases can be classified into two groups, i.e. periplasmic nitrate reductase (Nap) and membrane-bound nitrate reductase (Nar). The Nap enzyme, found mainly in the denitrifying purple bacteria, is a soluble protein with a heterodimeric composition. The large subunit (NapA) harbors a Mo-bis-molybdopterin guanine dinucleotide (Mo-bisMGD) complex and a [4Fe-4S] cluster, and the small subunit (NapB) is a diheme c protein that mediates internal electron transfer to the catalytic NapA subunit [25].

As compared with the Nap, the Nar enzyme is distributed more widely in the nitrate-respiring microorganisms including the Gram-negative and Gram-positive bacteria [24]. In general, the Nar complex is in the heterotrimeric configuration. In the *Escherichia coli* enzyme (NarGHI), which is the

most investigated Nar complex so far, the 145 kDa NarG subunit contains a Mo-bisMGD center for nitrate reduction, and the 60 kDa NarH subunit contains four iron-sulfur (Fe-S) clusters that function as internal electron mediators to the molybdopterin center in the NarG subunit. The NarG and NarH subunits are membrane-extrinsic, while the NarI subunit (20 kDa) is a hydrophobic membrane protein that harbors a protoheme moiety as the reaction site with quinol, a physiological electron donor to the NarGHI complex [21,26]. A three-dimensional structure of the whole Nar complex remains unknown due to the difficulty of crystallization of an amphipathic enzyme.

In archaea, purification of dissimilatory nitrate reductases has been reported from denitrifying halophiles in the genus *Haloferax* [3,5,14]. The *Haloferax* enzymes are membrane-bound, and found in heterodimeric or trimeric configurations. Their prosthetic groups have been rather poorly characterized, and so far detailed information regarding to their similarities to their bacterial counterparts is not available. Our previous study of the *Haloarcula marismortui* nitrate reductase identified the enzyme as a Nar-type enzyme for the first time, based on its catalytic features and its initial electron paramagnetic resonance (EPR) and chemical characterization of the molybdopterin center [31].

In this study, the gene encoding the *H. marismortui* nitrate reductase was cloned and sequenced. The deduced amino acid sequence of an archaeal Nar enzyme, reported for the first time, showed marked similarities with the bacterial counterparts, while there was a significant difference in the subcellular localization between the archaeal and bacterial enzymes. Moreover, the number and the types of the Fe-S clusters in the purified enzyme were investigated by X-band EPR spectroscopy.

2. Materials and methods

2.1. Purification and electrophoretic and enzymatic analysis

Purification of nitrate reductase from the denitrifying cells of *H. marismortui* ATCC43049 was carried out according to our previous report [31]. Sodium dodecyl sulfate-polyacrylamide gel electrophoresis (SDS-PAGE) was performed according to the method of Schägger and von Jagow [27]. Selenate-reducing activity of the purified enzyme was assayed on the native PAGE gel with potassium selenate instead of potassium nitrate [31].

2.2. Sequencing of the N-terminal and the internal peptides

The purified enzyme was denatured by treatment with 2% SDS and 2% β-mercaptoethanol for 5 min at 100°C, then loaded onto a Se-

*Corresponding author. Fax: (81)-54-238 0986.

E-mail address: sbtfuji@ipc.shizuoka.ac.jp (T. Fujiwara).

phacryl S-300 gel-filtration column (2×90 cm) equilibrated with 10 mM Tris–HCl buffer (pH 8.0) containing 0.1% SDS and 0.2 M NaCl. Subunits of the enzyme were collected separately, and their N-terminal amino acid sequences were analyzed using a protein sequencer model PPSQ-21 (Shimadzu Co., Kyoto, Japan).

Tryptic digestion of the purified enzyme was performed by treating 100 µg of the sample with 1 µg TPCK-trypsin in 50 mM (NH₄)HCO₃ containing 10 mM CaCl₂ for 24 h at 37°C. The peptide fragment mixtures thus obtained were fractionated by reverse-phase high performance liquid chromatography on a Cosmosil 5C18 packed column (4.6×250 mm; Tosoh Co., Tokyo, Japan) in 0.1% (v/v) trifluoroacetic acid with a linear gradient from 0 to 70% (v/v) acetonitrile. The fractionated fragments were lyophilized separately, dissolved in a minimum volume of 0.1% trifluoroacetic acid, and applied to the protein sequencer mentioned above.

2.3. Cloning of the gene encoding the enzyme

Extraction of the genomic DNA from the *H. marismortui* cells was performed as previously described [7]. Based on the amino acid sequences of two tryptic digests of the enzyme, GWE(D)(?)GGGW and LVNEYEVALPLHPEFR, three degenerated oligonucleotides (primer 1, 5'-GGGARGAYIIIGGNGGNGGNTGG-3'; primer 2, 5'-CG-RAAYTCNGGRTGNARNGG-3'; primer 3, 5'-GCNACYTCRT-AYTCRTTNAC-3', with R, Y, V, B, N representing A+G, C+T, A+C+G, C+G+T, A+C+G+T, respectively), were designed for the polymerase chain reaction (PCR)-amplification of the gene encoding the corresponding part of the enzyme. For the first amplification, primers 1 and 2 were used with the archaeal genomic DNA as the template. A mixture of the amplified fragments were then used as the template for the second PCR reaction with primers 1 and 3. The resulting 600 bp product was cloned into a pT7 Blue T vector (Novagen, Madison, WI, USA), and the nucleotide sequence was determined by the dideoxy chain termination method [8] using a DNA sequencer model 4200 (LI-COR Co., Lincoln, NE, USA). The deduced amino acid sequence of the 600 bp product was homologous with those of bacterial nitrate reductase genes.

Hybridization on *Sac*I-digested genomic DNA using the alkaline phosphatase-labeled 600 bp fragment as a DNA probe showed a single positive band corresponding to 2.7 kbp by using the chemiluminescent detection protocol (Amersham Pharmacia Biotech., Buckinghamshire, UK). The 2.7 kbp fragment was obtained from the *Sac*I-digested genomic DNA library, using standard DNA manipulation methods. Both strands of the obtained clone, designated pNR1, was fully sequenced. It contained two potent open reading frames, ORF-1 and ORF-2, although ORF-1 lacked its 5'-terminal portion. Therefore, by using the *Sac*I/*Bgl*II-digested 240 bp fragment prepared from pNR1 as a hybridization probe, the *Bgl*II/*Sma*I-digested genomic DNA library was screened to clone the DNA fragment expected to cover the 5'-region of the ORF-1. The 2.0 kbp fragment, designated pNR2, was cloned and sequenced. The resulting nucleotide sequence of 4500 bp, which covers the entire length of ORF-1 and ORF-2, was determined.

2.4. Subcellular localization of the enzyme

Localization of the active site of the *H. marismortui* nitrate reductase in the archaeal cells was estimated based on the reactivity of the enzyme with a membrane-permeable electron donor, benzylviologen radical (BV), as compared to that with a membrane-impermeable methylviologen radical (MV), as described by Jones and Garland [18] with the following modifications. *H. marismortui* cells grown in the denitrifying medium [31] and harvested in the early-exponential phase of the growth, were used as a suspension of the whole cells. The intactness of the cells was estimated by the level of the oxaloacetate-dependent oxidation of NADH (monitored spectrophotometrically at 340 nm) upon cell damage or lysis, due to leakage of the cognate cytoplasmic malate dehydrogenase (MDH) activity in the reaction mixture (100 mM Tris–HCl buffer (pH 7.5), 2.0 M NaCl, 0.1 mM NADH, 0.25 mM oxaloacetate, and 10 µg/ml protein). The broken cells were prepared by disruption of a portion of the whole cell suspension with a sonic oscillator and by removal of the unbroken cells by centrifugation at 15000×g for 10 min.

Nitrate reductase (Nar) activity was measured by mixing the whole or broken cell suspension of *H. marismortui* in the reaction mixture (100 mM Tris–HCl buffer (pH 7.5), 2.0 M NaCl, 10 mM NaNO₃, 2.3 mM dithionite and 0.12 mM BV or 0.2 mM MV, and 2 µg/ml protein).

For comparison, *E. coli* strain JM109 was cultivated anaerobically in the presence of nitrate [20], and the whole and broken cells were prepared as described by Jones and Garland [18]. Nar activity of *E. coli* was assayed essentially as described above, but in the absence of 2.0 M NaCl in the reaction mixture.

2.5. EPR measurements

EPR measurements were carried out using a JEOL JEX-RE1X spectrometer equipped with an Air Products model LTR-3 Heli-Tran cryostat system and a Scientific Instruments series 5500 temperature indicator/controller as reported previously [15,17]. All EPR data were processed using KaleidaGraph software ver. 3.05 (Abelbeck Software). The 7Fe form of zinc-containing ferredoxin was purified from *Sulfolobus tokodaii* strain 7 (formerly *Sulfolobus* sp. strain 7) as described previously [16] and was used as a control in the EPR measurements.

3. Results and discussion

3.1. Subunit structure

The nitrate reductase purified from *H. marismortui* displays a single band corresponding to a molecular mass of 63 kDa on a polyacrylamide gel when treated with 1 or 5% SDS at room temperature as shown in Fig. 1 (lanes 1 and 2). When the sample was treated with β-mercaptoethanol (lane 3) or at 100°C (lanes 4 and 5), two bands appeared accompanying the disappearance of the 63 kDa band. This indicates that the purified enzyme is composed of two subunits with the apparent molecular masses of 117 and 47 kDa, respectively, and that the 63 kDa band corresponds to an incomplete denaturation state of the purified enzyme. The N-terminal amino acid sequence of the larger (α) subunit was determined to be AVDDPIGSYP (with low recovery (2.8%) from the protein sequencer against the total mol of the applied sample), and that of the smaller (β) subunit could not be sequenced, probably owing to its modification at the N-terminus. The purified enzyme has a molecular weight of 208 000 [31] and contains 0.79 ± 0.07 mol of Mo, 10.7 ± 0.40 mol of Fe, and 10.4 ± 0.33

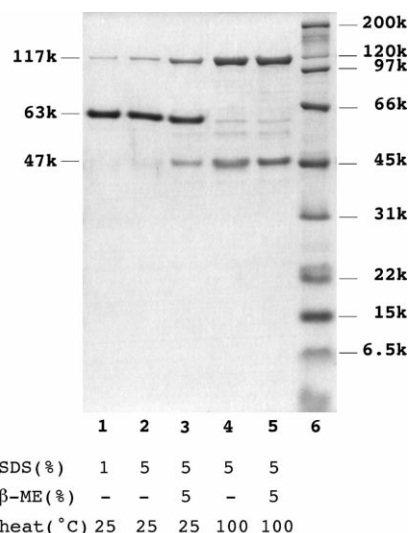


Fig. 1. SDS-PAGE of purified *H. marismortui* nitrate reductase. The pre-treatment conditions of the purified enzyme (1.6 µg) by SDS, β-mercaptoethanol (β-ME), and temperature are indicated in the figure (lanes 1–5). Standard proteins, with their molecular masses shown beside the gel, are in lane 6. Coomassie brilliant blue was used for protein-staining.

A.

HmNarG	msrndltdddegdsagis	rrdfvrglgaasllgatglsfaddgmdgleAVDDPIGSYPYRDWEDLYRD	67
EcNarG		MSKFLDRFRYFKQKGETFADGHGQLLNTNRDWEDGYRQ	38
TsSerA	mrkvmnspddngn	rrffllqfsmaalasaapssvwaFSKIQPIEDPLKSYPYRDWEDLYRK	61
EcDmsA		mktkipdavlaaevsrrglvkttaigglamassaltlpfsriaahVDSAIP	51
DdNapA		mstsrrdfikyfamsaavaaasgagfgslala	32
HmNarG	68	EWDWDSVARSTSVNCTGSCSWNVYVKDQGVWREEQAGDYPTFDESLPDPNPRG	CQKGACYTDYVNA 135
EcNarG	39	RWQHDKIVRSTGVNCTGSCSWKIYVKNGLVTWETQQTDPYRTRPDLNHEPRG	CPRGASYSWYLYS 105
TsSerA	62	EWTWSTGFITISNGCVAGCAWRVFKNGVPMREEQVSEYQLPG-VPDMNPRG	CQKGAIVCSWSKQ 327
EcDmsA	52	TKSDEKVIWSACTVNCGSRCLRMHVVDG--EIKYVETDNTGDDNYDGLHQVRA	CLGRSMRRRVYN 216
DdNapA	33	ADNRPEKWVKGVCRYCTGCGVLGVKDGKAVAIQGDPPN-----HNAGLLCL	LGKSLIPVLNS 91

B.

HmNarH	30	MDLNK	CIGCQTCTIA	CKNLWT	50	149	YLPRI	CNHCTHPS	CVEAC	PRSAI	171		
EcNarH	11	LNLDK	CIGCHTCSVT	CKNVWT	31	179	YLPRI	CEHCLNP	ACVAT	PSGAI	201		
TsSerB	10	FDLNK	CIGCHTCTMA	CKQLWT	30	128	YLPRI	CNHCSNP	ACLAACP	TKAI	150		
EcDmsB	9	IDSSR	CTGCKTCELA	CKDYKD	29	62	YLSIS	CNHCEDP	ACTKV	PSGAM	84		
			1 1 1 4					3 3 3 2					
HmNarH	182	VDQDR	CRGYRY	VEG	CPYKKV	202	209	KKSEK	CIFCYPRI	EGEGPDGET	FAPACAE	CPPLQR	244
EcNarH	212	IDQDK	CRGWRMCIT	G	CPYKKI	232	239	GKSEK	CIFCYPRI	EAG-----	OPTV	CSSETCVGRIR	268
TsSerB	161	VDQSR	CRGYRY	CVKA	CPYKGM	181	188	GTSEK	CIGCYPRI	VEK-----	EAPACVKQ	CSGRIR	217
EcDmsB	94	VDEDV	CIGCRY	CHMA	CPYGAP	114	121	GHMTK	CDG	CYDRVAEG-----	KKPI	CVESCPILRAL	150
			2 (2) 2 3					4 4			4 1		

Fig. 2. Sequence alignments of the *H. marismortui* NarG (A) and NarH (B). Sequences were aligned with counterpart bacterial nitrate reductases and structural relatives using the CLUSTALW alignment algorithm [29]. A: Putative signal sequences are shown by lower case letters, and twin-arginine motifs are boxed. Shaded residues highlight the N-terminal consensus motif -(Cys/His)-Xaa₃-Cys-Xaa₃-Cys-/-Cys-. In *E. coli* Nar, a mutant NarG subunit, in which the consensus His (His⁵⁰) is replaced by Cys, does not show any additional EPR signal in the *g*=2 region [22]. On the other hand, site-directed mutagenesis of the second Cys of this motif in *E. coli* DmsA by Ala or Ser promotes assembly of an extra [3Fe-4S] cluster in close proximity to the Mo-bisMGD center [9]. Amino acids are numbered in the margins. B: Cys residues in the putative Fe-S cluster-binding motifs are shaded. Numbers (1–4) under the conserved Cys residues correspond to the numbering of the possible arrangements of the four Fe-S clusters in the *E. coli* NarH protein proposed by Guigliarelli et al. [12]. HmNarGH, *H. marismortui* NarGH (accession number EMBL AJ277440); EcNarGH, *E. coli* NarGH (GenBank X16181); TsSerAB, *T. selenatis* SerAB (EMBL AJ007744); EcDmsAB, *E. coli* DmsAB (GenBank J03412); DdNapA, *D. desulfuricans* NapA (GenBank Y18045).

mol of acid-labile sulfur atoms per mol of the enzyme (based on our previous report [31]), indicating its probable subunit composition to be $\alpha_1\beta_1$. These results suggest that one Mo-cofactor and multiple Fe-S clusters (up to four clusters per Mo) exist in the archaeal enzyme.

3.2. Cloning and nucleotide sequence analysis

The plasmid clones pNR1, pNR2 and their 13 subclones were used to determine the nucleotide sequence of a DNA stretch starting with the first basepair of a *Sma*I site and ending with the last basepair of a *Sac*I site. The resulting sequence of 4500 bp contained two complete ORFs as described in Section 2. ORF-1, which starts at nucleotide 545 and ends at nucleotide 3403, encodes a product of 952 amino acid residues with an estimated molecular weight of 107743. The stop codon of ORF-1 overlaps with the start codon of ORF-2 (nucleotides 3400–4476), which encodes a product of 358 residues with an estimated molecular weight of 41121. The N-terminal amino acid sequence of the larger subunit was identical with a part of the deduced sequence of ORF-1 (see Fig. 2A). Further, the amino acid sequences of the two tryptic digests matched the corresponding deduced inner sequences of ORF-2. These results demonstrate that the two ORFs represent the genes encoding the large and small subunits of the *H. marismortui* enzyme, respectively. Nucleotide and amino acid sequence data are available under accession number AJ277440 in the EMBL nucleotide sequence database.

3.3. Multiple amino acid sequence alignments and subcellular localization

The deduced amino acid sequences of ORF-1 and ORF-2 showed overall homologies with those of the NarG and NarH subunits of *E. coli* Nar enzyme (34.8 and 42.7% identities, respectively). Therefore, ORF-1 and ORF-2 were designated narG and narH, respectively. Interestingly, in addition to other bacterial NarGH enzymes, *H. marismortui* NarGH enzyme also shows a significant structural similarity to *Thauera selenatis* dissimilatory selenate reductase (Ser), which is a terminal enzyme in bacterial anaerobic selenate respiration that catalyzes the reduction of selenate with a concomitant production of selenite [19,28]. The amino acid sequences of SerA (918 residues) and SerB (327 residues) subunits of the *T. selenatis* selenate reductase could be aligned with those of *H. marismortui* NarG and NarH proteins with a few sequence gaps (30.8 and 47.8% identities, respectively). However, the purified *H. marismortui* NarGH enzyme did not reduce selenate, indicating its distinctive substrate specificity.

As shown in Fig. 2A, the typical signal peptide containing a twin-arginine motif and the following hydrophobic stretch (-GLGAASLLGA-) are found in the N-terminal region of *H. marismortui* NarG [23]. Similar signal peptides in the N-termini of the catalytic subunits of several other related enzymes are known to determine the localization of the enzymes relative to the cytoplasmic membrane, and the catalytic site of *T. selenatis* SerA [28] has been shown to be located on the periplasmic side on the basis of subcellular fractionation ex-

Table 1
Reactivities of MV and BV with nitrate reductase in the whole and broken cells of *H. marismortui*

		NaR activity ($\mu\text{mol}/\text{min}/\text{mg}$ protein)			MDH activity ($\mu\text{mol}/\text{min}/\text{mg}$ protein)
		MV	BV	–	
<i>H. marismortui</i>	whole cells	4.01	3.38	0.05	0.00
	broken cells	3.89	3.40	0.02	0.53
<i>E. coli</i>	whole cells	0.30	2.80	0.05	n.d.
	broken cells	2.47	3.59	0.03	n.d.

The subcellular localization of the catalytic site of *H. marismortui* Nar enzyme was performed as described in Section 2. n.d., not determined.

periments. The subcellular localization experiments with the intact *H. marismortui* cells (see Section 2) clearly show that the archaeal Nar enzyme can react with both membrane-impermeable MV and membrane-permeable BV in situ (Table 1). On the other hand, *E. coli* NarG does not possess any signal sequence (Fig. 2A) and has been shown to be located on the cytoplasmic side of the membrane [21] as it does not react with MV in situ (Table 1). Hence, we suggest that the N-terminal signal peptide of *H. marismortui* NarG also deter-

mines the localization of the catalytic site of the native Nar complex in the periplasmic side of the archaeal membrane.

In Fig. 2, the deduced amino acid sequences in the N-terminal region of *H. marismortui* NarG (Fig. 2A) and in the internal regions of the NarH involved in the possible Fe–S cluster binding motif (Fig. 2B) were aligned with the equivalent regions of several Mo-bisMGD-containing enzymes, including *E. coli* Nar, *T. selenatis* Ser, *E. coli* dimethylsulfoxide reductase (Dms), and *Desulfovibrio desulfuricans* Nap. A possible [4Fe–4S] cluster binding motif with the complete cysteine ligations was identified at the N-terminal part of *E. coli* DmsA and *D. desulfuricans* NapA (Fig. 2A). Similar motifs were also present in *H. marismortui* NarG, *E. coli* NarG and *T. selenatis* SerA, but, in these cases, they are incomplete, as the first Cys in the motif is replaced by His, and may not serve as ligands to a [3Fe–4S]/[4Fe–4S] cluster [22]. In Fig. 2B, the deduced sequence of *H. marismortui* NarH clearly indicates the presence of one regular [3Fe–4S] and three [4Fe–4S] cluster binding motifs that are equivalent to those previously reported for *E. coli* NarH [6]. The site-directed mutagenesis studies on the *E. coli* enzyme have suggested possible pairs of the cysteine motifs for the cluster ligations (groups 1–4) as indicated in Fig. 2B [12].

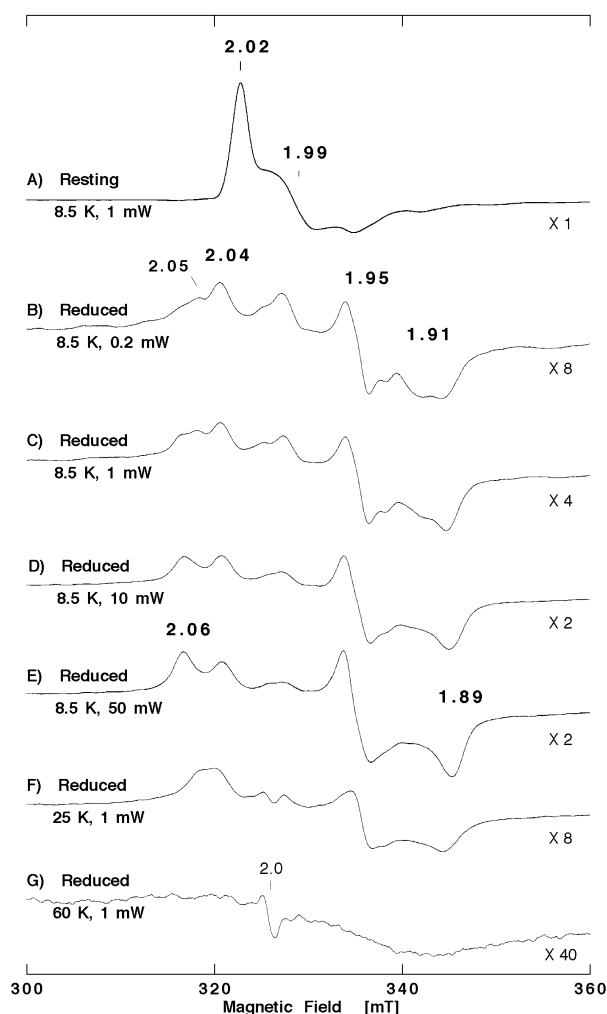


Fig. 3. EPR spectra of *H. marismortui* nitrate reductase NarGH at 8.5–60 K. Spectra (A) and (B–G) are of the oxidized and dithionite-reduced enzyme, respectively. The samples were produced in 6.3 mg protein/ml in 100 mM Tris–HCl buffer (pH 7.8). In the *E. coli* Nar enzyme, the equivalent EPR-visible Fe–S clusters in the $g=2$ region have been reported to be associated with the NarH subunit [12]. Modulation amplitude, 1.0 mT; microwave power, temperature, g values, and relative gain are indicated in the figure.

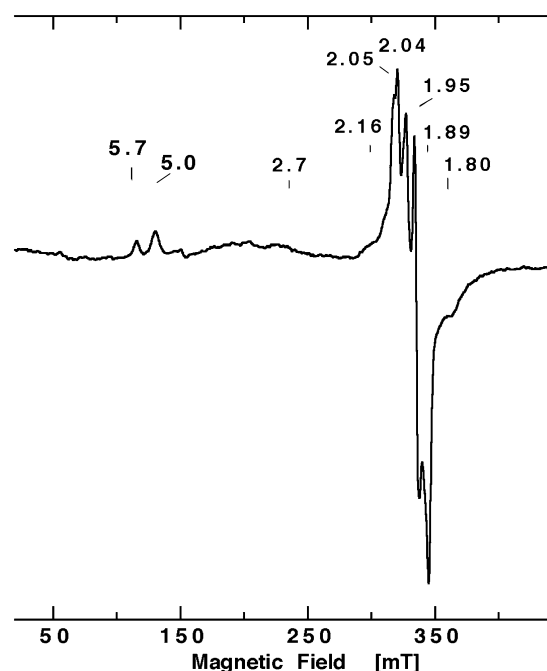


Fig. 4. Low-field resonances in the EPR spectrum of dithionite-reduced *H. marismortui* nitrate reductase. Modulation amplitude, 1.0 mT; microwave power, 1 mW; temperature, 8.5 K. The g values are indicated in the figure.

3.4. EPR spectroscopic analysis

In agreement with the results inferred by the sequence and metal content analyses of *H. marismortui* nitrate reductase, the EPR spectra of the oxidized enzyme showed a sharp peak at $g=2.02$ and a trough at $g=1.99$, which are characteristic of a $[3\text{Fe-4S}]^{1+}$ cluster (Fig. 3A). Dithionite-reduced enzyme showed complex features consisting mainly of EPR signals at $g=2.06$, 2.05, 2.04, 1.95, 1.91 and 1.89 (Fig. 3B–E), with additional broad wing-like features at 8.5 K (Fig. 4). These EPR signals are substantially broadened at temperatures above 20 K (Fig. 3F, G), and hence have the characteristics of $S=1/2[4\text{Fe-4S}]^{1+}$ clusters. The broad outer lines at 8.5 K of the reduced enzyme indicate spin–spin interactions between adjacent $[3\text{Fe-4S}]$ and/or $[4\text{Fe-4S}]$ clusters, as found in regular 8Fe- and 7Fe-containing dicluster ferredoxins [17]. The modifications of the g_z and g_y signals on application of different amounts of microwave power and temperatures are consistent with the presence of at least three $[4\text{Fe-4S}]$ clusters, although the spectrum of the interacting pair of the reduced clusters lacks some of the features of the spectra of individual clusters. Double integration of the $S=1/2$ resonances of the oxidized and reduced *H. marismortui* enzyme suggested the presence of approximately one $[3\text{Fe-4S}]$ cluster and three $[4\text{Fe-4S}]$ clusters, as found in *E. coli* Nar [11,12] and as expected from the sequence features of *H. marismortui* NarH (Fig. 2B). These four Fe–S clusters may mediate intramolecular electron transfer between a physiological electron donor and the Mo-bisMGD center in the archaeal enzyme.

In addition to the spectral contribution of multiple, spin-coupled $S=1/2$ species in the $g=2$ region and a broad and weak low-field resonance associated with an $S=2[3\text{Fe-4S}]^0$ cluster, the EPR spectrum of the dithionite-reduced *H. marismortui* enzyme exhibited an additional broad EPR feature at $g=5.7$, 5.0 and ~ 2.7 in the low field region (Fig. 4). This was not observed with the 7Fe form of the dithionite-reduced zinc-containing ferredoxin from *S. tokodaii* strain 7 containing one $[3\text{Fe-4S}]$ cluster and one $[4\text{Fe-4S}]$ cluster [17] (data not shown). This species was not observed with the oxidized *H. marismortui* enzyme (data not shown), and is therefore likely to be associated with a putative $S=3/2[4\text{Fe-4S}]^{1+}$ cluster [1,13]. Since the low-field EPR resonance has not been investigated in *E. coli* Nar or Dms, it is currently not known if this center is unique to the reduced archaeal enzyme. Further studies (including low-temperature magnetic circular dichroism and Mössbauer spectroscopies) will allow its detailed assignment and its possible correlation with the consensus Cys groups in *H. marismortui* NarGH (Fig. 2).

In this study, we demonstrate that archaeal nitrate reductase from *H. marismortui* is composed of two subunits, NarG and NarH, which have homologs in the bacterial domain, and that it contains one $[3\text{Fe-4S}]$ and at least three $[4\text{Fe-4S}]$ clusters, in addition to the catalytic Mo-bisMGD center characterized previously [31]. The results are consistent with our earlier report that the archaeal enzyme shows chlorate-reducing activity that is characteristic of the bacterial Nar enzymes [31], and lend some credence to our proposal that they might have evolved from a common ancestral soluble enzyme.

Our on-going sequence analysis of the archaeal *nar* gene cluster further suggests that the purified NarGH probably represents a minimal functional and structural module of a larger membrane protein complex. We found several additional ORFs downstream of the *narGH* genes (EMBL accession

number AJ429077), and assigned two genes encoding the archaeal homologs of bacterial NarJ (a putative chaperon-like protein involved in the Mo-pterin cofactor assembly) and *T. selenatis* SerC (a putative cytochrome *b* subunit of the bacterial selenate reductase). On the other hand, no *narI* gene was found. We therefore suggest that the native *H. marismortui* dissimilatory Nar complex is phylogenetically and perhaps structurally closely related to the *T. selenatis* Ser complex, having the common catalytic site topology relative to the membrane (Table 1) and the SerC-like cytochrome *b* anchor. Intriguingly, another archaeal nitrate reductase complex purified from the cytoplasmic membrane of a hyperthermophilic crenarchaeote *Pyrobaculum aerophilum* [2] is also a molybdoenzyme having the *b*-type cytochrome, of which the sequence shows similarity to the *T. selenatis* SerC. It seems plausible to postulate that these archaeal Nar complexes may represent a novel class of the membrane-bound Nar enzymes, reflecting their unique evolutionary consequences.

The purified *H. marismortui* NarGH does not have the ability to oxidize quinol, a potential physiological electron donor to the bacterial Nar, nor does it contain any cytochrome *b* subunit that could mediate the intermolecular electron transfer from quinol to the Fe–S centers in NarH. The sequence information and the presence of the multiple membrane-bound *b*-type cytochromes in several halophilic archaea [10] (Yoshimatsu, K., unpublished results) suggest that additional SerC-like *b*-type cytochrome subunit, probably dissociated from the halophile Nar complex during the purification, is required for the physiological function. Further attempts to isolate the whole *H. marismortui* Nar complex are in progress.

Acknowledgements: We thank Dr. H. Taguchi (Research Laboratory of Resources Utilization, Tokyo Institute of Technology) for the protein sequence analysis, and Dr. K. Tamura and Dr. T. Iizuka (The Institute of Physical and Chemical Research) for allowing us to utilize the EPR facility. This work was supported in part by Saneyoshi Foundation Grant 1320 (to T.F.) and Japan–United States Cooperative Science Program Grant JSPS BSAR-507 (to T.I.).

References

- [1] Adams, M.W.W. (1992) Adv. Inorg. Chem. 38, 341–396.
- [2] Afshar, S., Johnson, E., de Vries, S. and Schöörder, I. (2001) J. Bacteriol. 183, 5491–5495.
- [3] Alvarez-Ossorio, M.C., Muriana, F.J.G., de la Rosa, F.F. and Relimpio, A.M. (1992) Z. Naturforsch. 47C, 670–676.
- [4] Antipov, A.N., Lyalikova, N.N., Khijniak, T.V. and L'vov, N.P. (1998) FEBS Lett. 441, 257–260.
- [5] Bickel-Sandkötter, S. and Ufer, M. (1995) Z. Naturforsch. 50C, 365–372.
- [6] Blasco, F., Iobbi, C., Giordano, G., Chippaux, M. and Bonnefoy, V. (1989) Mol. Gen. Genet. 218, 249–256.
- [7] Blin, N. and Stafford, D.W. (1976) Nucleic Acids Res. 3, 2303–2308.
- [8] Chen, E.Y. and Seeburg, P.H. (1985) DNA 4, 165–170.
- [9] Dias, J.M., Than, M.E., Humm, A., Huber, R., Bourenkov, G.P., Bartunik, H.D., Bursakov, S., Calvete, J., Caldeira, J., Carneiro, C., Moura, J.J., Moura, I. and Romao, M.J. (1999) Struct. Fold Des. 7, 65–79.
- [10] Fujiwara, T., Fukumori, Y. and Yamanaka, T. (1993) J. Biochem. 113, 48–54.
- [11] Guigliarelli, B., Asso, M., More, C., Augier, V., Blasco, F., Pommer, J., Giordano, G. and Bertrand, P. (1992) Eur. J. Biochem. 207, 61–68.
- [12] Guigliarelli, B., Magalon, A., Asso, M., Bertrand, P., Frixon, C., Giordano, G. and Blasco, F. (1996) Biochemistry 35, 4828–4836.
- [13] Hagen, W.R. (1992) Adv. Inorg. Chem. 38, 165–222.

- [14] Hochstein, L.I. and Lang, F. (1991) *Arch. Biochem. Biophys.* 288, 380–385.
- [15] Iwasaki, T., Wakagi, T., Isogai, Y., Tanaka, K., Iizuka, T. and Oshima, T. (1994) *J. Biol. Chem.* 269, 29444–29450.
- [16] Iwasaki, T. and Oshima, T. (2001) *Methods Enzymol.* 334, 3–22.
- [17] Iwasaki, T., Watanabe, E., Ohmori, D., Imai, T., Urushiyama, A., Akiyama, M., Hayashi-Iwasaki, Y., Cosper, N.J. and Scott, R.A. (2000) *J. Biol. Chem.* 275, 25391–25401.
- [18] Jones, R.W. and Garland, P.B. (1977) *Biochem. J.* 164, 199–211.
- [19] Krafft, T., Bowen, A., Theis, F. and Macy, J.M. (2000) *DNA Seq.* 10, 365–377.
- [20] Lester, R.L. and DeMoss, J.A. (1971) *J. Bacteriol.* 105, 1006–1014.
- [21] MacGregor, C.H. and Christopher, A.R. (1987) *Arch. Biochem. Biophys.* 185, 204–213.
- [22] Magalon, A., Asso, M., Guigliarelli, B., Rothery, R.A., Bertrand, P., Giordano, G. and Blasco, F. (1998) *Biochemistry* 37, 7363–7370.
- [23] Nielsen, H., Engelbrecht, J., Brunak, S. and von Heijne, G. (1997) *Protein Eng.* 10, 1–6.
- [24] Richardson, D.J., Berks, B.C., Russel, D.A., Spiro, S. and Taylor, C.J. (2001) *Cell. Mol. Life Sci.* 58, 165–178.
- [25] Richardson, D.J., McEwan, A.G., Page, M.D., Jackson, J.B. and Ferguson, S.J. (1990) *Eur. J. Biochem.* 194, 263–270.
- [26] Rothery, R.A., Blasco, F. and Weiner, J.H. (2001) *Biochemistry* 40, 5260–5268.
- [27] Schägger, H. and von Jagow, G. (1987) *Anal. Biochem.* 166, 368–379.
- [28] Schörder, I., Rech, S., Krafft, T. and Macy, J.M. (1997) *J. Biol. Chem.* 272, 23765–23768.
- [29] Thompson, J.D., Higgings, D.G. and Gibson, T.J. (1994) *Nucleic Acids Res.* 22, 4673–4680.
- [30] Trieber, C.A., Rothery, R.A. and Weiner, J.H. (1996) *J. Biol. Chem.* 271, 4620–4626.
- [31] Yoshimatsu, K., Sakurai, T. and Fujiwara, T. (2000) *FEBS Lett.* 470, 200–216.
- [32] Zumft, W.G. (1997) *Microbiol. Mol. Biol. Rev.* 61, 533–616.